*AAPS PharmSciTech, Vol. 16, No. 3, June 2015 (© 2014)*
DOI: 10.1208/s12249-014-0222-8

*Research Article*

# The Influence of Secondary Processing on the Structural Relaxation Dynamics of Fluticasone Propionate

**Roberto Depasquale,[1] Sau L. Lee,[2] Bhawana Saluja,[3] Jagdeep Shur,[1] and Robert Price[1,4]**

*Received 11 June 2014; accepted 12 September 2014; published online 15 November 2014*

***ABSTRACT.*** This study investigated the structural relaxation of micronized fluticasone propionate (FP) under different lagering conditions and its influence on aerodynamic particle size distribution (APSD) of binary and tertiary carrier-based dry powder inhaler (DPI) formulations. Micronized FP was lagered under low humidity (LH 25 C, 33% RH [relative humidity]), high humidity (HH 25°C, 75% RH) for 30, 60, and 90 days, respectively, and high temperature (HT 60°C, 44% RH) for 14 days. Physicochemical, surface interfacial properties *via* cohesive-adhesive balance (CAB) measurements and amorphous disorder levels of the FP samples were characterized. Particle size, surface area, and rugosity suggested minimal morphological changes of the lagered FP samples, with the exception of the 90-day HH (HH90) sample. HH90 FP samples appeared to undergo surface reconstruction with a reduction in surface rugosity. LH and HH lagering reduced the levels of amorphous content over 90-day exposure, which influenced the CAB measurements with lactose monohydrate and salmeterol xinafoate (SX). CAB analysis suggested that LH and HH lagering led to different interfacial interactions with lactose monohydrate but an increasing adhesive affinity with SX. HT lagering led to no detectable levels of the amorphous disorder, resulting in an increase in the adhesive interaction with lactose monohydrate. APSD analysis suggested that the fine particle mass of FP and SX was affected by the lagering of the FP. In conclusion, environmental conditions during the lagering of FP may have a profound effect on physicochemical and interfacial properties as well as product performance of binary and tertiary carrier-based DPI formulations.

**KEY WORDS:** cohesive-adhesive balance; laagering; mechanical activation; particle adhesion; process-induced structural disorder.

## INTRODUCTION

Particle size reduction of active pharmaceutical ingredients (APIs) for delivery to the lungs requires secondary processing of primary crystals using highly energetic comminution techniques, such as air-jet micronization (1). For brittle materials, particle-particle and particle-wall collisions within a micronizer often lead to the formation of short-lived defects formed along existing flaws within a crystalline lattice that can lead to crystal fracture (2,3). However, at the brittle-ductile transition, the material absorbs a significant amount of impact energy before undergoing any further particle reduction (4). This impact energy is stored as strain energy within the crystalline lattice in the form of structural defects, dislocations, and, at the limit, can lead to localized amorphous regions on a particle surface (4–6).

Process-induced structural disorder can lead to uncontrolled thermodynamic changes to the materials and is commonly described as "mechanical activation" (4–7). Mechanical activation may directly influence the physicochemical properties of a substance, for example, surface free energy, reactivity, conductivity, and true density (6,8). For carrier-based dry powder inhaler (DPIs) formulations, mechanical activation can directly influence the interfacial free energy of the respirable drug particles (*e.g.*, <5 μm), which may increase the tendency for agglomeration. This may also affect the relative magnitude of the cohesive (drug-drug) and adhesive (drug-excipient) interparticulate forces. Since the performance of adhesive mixtures is a function of the relative magnitude of these forces, the interfacial properties of secondary processed APIs can dominate blending dynamics, formulation microstructure, and ultimately drug product quality and performance of carrier-based DPI formulations (6).

**Electronic supplementary material** The online version of this article (doi:10.1208/s12249-014-0222-8) contains supplementary material, which is available to authorized users.

[1] Pharmaceutical Surface Science Research Group, Department of Pharmacy & Pharmacology, University of Bath, Bath, BA2 7AY, UK.
[2] Office of Pharmaceutical Science, Center for Drug Evaluation and Research, U.S. Food and Drug Administration, White Oak Building 51, 10903, New Hampshire Avenue, Silver Spring, Maryland 20993, USA.
[3] Office of Generic Drugs, Center for Drug Evaluation and Research, U.S. Food and Drug Administration, White Oak Building 75, 10903, New Hampshire Avenue, Silver Spring, Maryland 20993, USA.
[4] To whom correspondence should be addressed. (e-mail: r.price@bath.ac.uk )

 

Mechanically activated particles are thermodynamically unstable and are driven to undergo structural relaxation to a more stable state (4,5). Structural relaxation kinetics has been shown to be strongly dependent on environmental conditions (temperature and relative humidity), which may influence the degree of molecular mobility within the material, and the period of exposure to such conditions (5,6). The lagering or quarantine period required for materials to undergo structural relaxation may vary significantly from minutes, hours to months and appears to be highly dependent on their hydrophilic/hydrophobic nature (4,6).

Accelerated stability conditions of both temperature and relative humidity have been shown to expedite the rate of structural relaxation and may aid in the stabilization of particulate surfaces upon secondary processing (6,9). Studies have also shown that post-micronization relaxation may significantly reduce the levels of localized amorphous disorder and the tendency for micronized particles to aggregate (9). The use of post-micronization environmental conditioning appears to be widely applied to hydrophilic compounds (10–12). For example, micronized tiotropium bromide monohydrate was exposed to the conditions of 70–80% RH (relative humidity) and 25–30°C for up to 28 h on sheet metal racks prior to formulating as a DPI product (10). The structural relaxation of the conditioned tiotropium bromide monohydrate is characterized by measuring the change in specific enthalpy of solution. Micronized salbutamol sulfate was mechanically relaxed to a low energy, crystalline form for use in suspension-based metered dose inhalers (MDIs) by exposing a shallow bed of powder to the conditions of 60% RH and 25°C for 65 h (11). Micronized glycopyrrolate bromide could be exposed to a dry environment at an elevated temperature between 60 and 90°C for at least 6 h, but preferably between 24 and 50 h, to limit the tendency of the particles to aggregate and/or agglomerate upon storage of the DPI formulation (12).

For hydrophobic drugs, there is limited literature regarding the use of environmental conditions for post-micronization surface conditioning of materials. Among these, Joshi *et al.* showed an interesting observation on temperature-dependent stress relaxation of budesonide that led to an anomalous increase in specific surface area during post-micronization storage (3). The significant increase in surface area of budesonide upon storage was hypothesized to be related to the residual stress stored in the form of defects and dislocation upon micronization, which may lead to crack propagation and induce secondary particle fracture with the creation of new surface (3).

Based on the above information, the properties of carrier-based DPI formulation prepared with the freshly micronized or lagered (post-micronization and conditioned) drug are likely to be different, particularly as its performance is strongly dependent on the particle size, morphology, and interfacial chemistry of the particle surface (6). Any processing or storage conditions that may affect such properties need to be monitored and controlled to ensure formulation consistency during processing and over the product shelf life. Therefore, the aim of this study is to investigate the structural relaxation of micronized fluticasone propionate (FP) stored under different conditions of temperature and relative humidity and their possible influence on the FP physicochemical and interfacial properties. FP was chosen due to its hydrophobic nature and our limited understanding of the structural relaxation kinetics of such hydrophobic materials. The results of this study are expected to provide a valuable insight into how changes to these material properties during relaxation affect cohesive forces (FP-FP), adhesive forces with another drug component such as salmeterol xinafoate (SX) and lactose monohydrate, and consequently the *in vitro* performance of carrier-based DPI formulations.

## MATERIALS AND METHODS

### Materials

Micronized FP ($C_{25}H_{31}F_3O_5S$, molecular weight = 500.571) was purchased from Chemagis (Lot no. 104364, 100 g, Bnei Brak, Israel). The FP sample was shipped directly upon micronization and supplied in very tight packaging and held under 10% RH during transport. Salmeterol xinafoate ($C_{36}H_{45}NO_7$, molecular weight = 603.745) was sourced from Neuland Pharmaceuticals (Lot no. 12004, 20 g, Mumbai, India). A milled grade (ML001) of lactose monohydrate was sourced from DFE Pharma (Lot no. 10474128, Borculo, Netherlands). *In vitro* aerosolization testing of the binary and combination DPI formulations was performed using a Cipla Rotahaler® DPI capsule device (Cipla, Mumbai, India). Water used during the studies was Milli-Q reverse osmosis purified (Merck Millipore, Darmstadt, Germany). Methanol, acetone, and acetonitrile were of HPLC grade and purchased from Sigma (Gillingham, UK).

### Methods

A 2-g sample of FP was taken from a micronized batch for full physicochemical characterization. The remaining drug sample was separated into three 6-g batches and conditioned under three different environmental conditions of temperature and relative humidity for well-defined periods. An aged batch of micronized SX (>12 months) was used for tertiary DPI formulation preparations and was kept under ambient conditions during the period of the study. The use of such aged SX batch allowed the investigation to focus on examining the effect of FP relaxation behavior under different storage conditions on the *in vitro* performance of the tertiary DPI formulation, as its physicochemical and interfacial properties were not expected to change. The particle size distribution of the coarse lactose monohydrate was monitored during the study to ensure that there was no change in particle size, since any change to the fine or coarse end of the particle size distribution may influence drug product performance.

#### *Conditioning of Micronized FP*

The three conditioning environments chosen for this investigation were (1) ambient temperature and low humidity (LH) (25°C, 33% RH), (2) ambient temperature and high humidity (HH) (25°C, 75% RH), and (3) high temperature and ambient humidity (HT) (60°C, 44% RH). An aliquot of each conditioned FP sample (2 g) was taken from the LH and HH conditions upon being lagered for 30, 60, and 90 days. The HT sample was quarantined at a single time point of 14 days. All samples were sieved through a 500-μm mesh sieve prior to physicochemical characterization. Table I provides a summary

**Table I.** Nomenclature of Post-micronized FP Samples Based on Their Conditioning Environments and Periods

| Conditioning environment | Conditioning period (day) | Sample reference |
|---|---|---|
| Micronized (used as received) | 0 | Day 0 |
| 25°C, 33% RH | 30 | LH30 |
| | 60 | LH60 |
| | 90 | LH90 |
| 25°C, 75% RH | 30 | HH30 |
| | 60 | HH60 |
| | 90 | HH90 |
| 60°C, 44% RH | 14 | HT |

*RH* relative humidity, *LH* low humidity, *HH* high humidity, *HT* high temperature

of the conditioning environments and periods for micronized FP samples as well as their corresponding nomenclatures.

*Laser Diffraction*

Particle size distributions (PSDs) of all FP samples were measured in the wet state using a Sympatec HELOS and CUVETTE (Sympatec GmbH, Clausthal-Zellerfeld, Germany) laser diffraction system using an R3 lens (0.5–175 μm). Approximately 10 mg of FP was suspended in HPLC-grade cyclohexane containing 0.5% *w*/*v* lecithin (Acros Organics, Geel, Belgium) and sonicated for 5 min and then immediately transferred into a 50-mL cuvette to produce an appropriate optical concentration (8–12%). Each measurement was performed in triplicate. Particle size analysis was performed using WINDOX 5.0 software (Sympatec GmbH, Clausthal-Zellerfeld, Germany).

*Scanning Electron Microscopy*

Particle morphology of all FP samples was investigated using scanning electron microscopy (SEM). Sample aliquots were fixed onto sticky carbon tabs (Agar Scientific, Cambridge, UK), followed by removal of excess powder using pressurized air. Samples were subsequently sputter coated with gold (Edwards Sputter Coater S150B, Edwards High Vacuum, Sussex, UK) to achieve a thickness of approximately 20 nm. Imaging was performed using a scanning electron microscope (JEOL JSM6480LV, Tokyo, Japan) using 15-kV accelerating voltage.

*X-ray Powder Diffraction*

The X-ray powder diffraction (XRPD) patterns of FP samples were analyzed by a Bruker Powder Diffractometer (D8; Bruker AXS Inc., Madison, USA) using CuKα radiation ($\lambda$=1.54 Å). The data were collected over a single 2θ sweep with a range of 2θ=4–60° and a step size of 0.025°/step with a step time of 1.5 s.

*Differential Scanning Calorimetry*

The thermal properties of all samples were investigated using a differential scanning calorimeter (DSC 2920, TA Instruments, Surrey, UK), calibrated with an indium standard. Approximately 3 mg of sample was accurately weighted into an aluminum pan and crimped with a lid to form a hermetic seal. The sample and reference pan were heated at a rate of 10°C/min from 30 to 350°C. The calorimeter head was continuously flushed with dry nitrogen gas at 0.2 L/min during all measurements.

*Specific Surface Area by Brunauer-Emmett-Teller*

The specific surface area (SSA) of FP samples was measured using a Gemini 2360 surface area analyzer (Micromeritics Instrument Corporation, Norcross, USA). A five-point Brunauer-Emmett-Teller (BET) nitrogen adsorption analysis was carried out in triplicate after degassing the samples for 24 h in a FlowPrep 060 degasser (Micromeritics Instrument Corporation, Norcross, USA).

*Rugosity*

Rugosity ($R_a$) is a semiquantitative measure of shape and surface texture of particles and can be calculated based on the ratio of the surface area calculated by BET (SSA) to a product of the drug density and the surface area by laser diffraction ($S_v$) (3). As described above, the laser diffraction measurement assumes that particles are smooth and spherical and does not account for the surface roughness or shape of particles in its theoretically calculated surface area. Thus, $R_a$ can provide an estimate of changes that could be attributed to surface texture and smoothness.

*Thermal Activity Monitoring*

Calorimetric data were recorded using a 2277 Thermal Activity Monitor (TAM, Thermometric AB, Jarfalla, Sweden) at 25°C equipped with a gas perfusion unit. Briefly, the unit controls the relative humidity of a carrier gas flowing over the sample by proportional mixing of two gas lines (0 and 100% RH) using independent mass-flow controllers. This allows freshly loaded samples to be initially held under a dry atmosphere, limiting humidity induced relaxation of amorphous disorder present and allowing the apparatus to reach thermal equilibrium before the commencement of data capture. Data were recorded every 10 s with an amplifier range of 3000 μW using the dedicated software package Digitam 4.1. For the FP analysis, the RH program was initially set to 0% RH for 3 h and then switched to 90% RH for a minimum of 12 h and subsequently returned to 0% RH once the heat signal returned to baseline. All data were recorded in triplicate. Peak analysis was performed using Origin (Microcal Software Inc., USA). In all cases, the drying response was subtracted from the wetting response to record the overall heat activity that was then used to record the enthalpy difference. These enthalpy values were then used to calculate the amorphous content of the samples by means of calibrated enthalpy curves of 100% crystalline and 100% amorphous FP.

### Cohesive-Adhesive Balance

*Preparation of Crystal Substrates*

To perform quantitative scanning probe microscopy (SPM) measurements of the cohesive-adhesive balance (CAB) of the FP samples, smooth single crystal surfaces of FP, SX, and lactose monohydrate were prepared (13) (1). The procedure for these preparations is briefly summarized below.

A saturated solution of FP in 2 mL of acetone was prepared and sonicated prior to filtration *via* a 0.22-μm polytetrafluoroethylene (PTFE) membrane filter (Whatman Inc., Clifton, NJ, USA). FP was crystallized using water as an anti-solvent. Specifically, a microscope cover slip (12 mm× 12 mm) was supported on a vertical post in a crystallization dish that contained the anti-solvent. A droplet of the FP-saturated solution was placed on the coverslip using a syringe attached to the 0.22-μm-membrane filter. The system was sealed by inverting a glass lid in the crystallization dish to allow vapor phases of the miscible solvents to come into equilibrium, resulting in heterogeneous nucleation and crystal growth within the solution droplet. A similar approach was used for the preparation of smooth crystal substrates of lactose monohydrate and SX and a detailed method is published elsewhere (1).

### Interaction Force Measurements

Prior to force measurements, individual particles from each sample of FP were attached onto standard V-shaped tipless cantilevers with pre-defined spring constants (DNP-020, DI, CA, USA) using an epoxy resin glue (Araldite, Cambridge, UK). Five probes were prepared for the initial, LH, HH, and HT conditioned FP samples at each pre-defined lagering period. All probes were examined with an optical microscope (magnification ×50) to ensure the integrity of the attached particle before allowing the thin layer of glue to cure and dry.

Single crystal substrates were loaded onto the scanner stage of a multimode scanning probe microscope (SPM) (Bruker, Santa Barbara, CA, USA), which was enclosed in a custom-built environmental chamber, in which the ambient conditions were maintained at a constant temperature of 25°C (±1.5°C) and relative humidity of 44% RH (±3%). The interaction forces were measured by recording the deflection of a cantilever as a function of the substrate displacement ($z$) by applying Hooke's law. Individual force curves ($n$=1024) were conducted over a 10 μm×10 μm area at a scan rate of 4 Hz and a compressive load of 40 nN.

A custom-built software was developed to extract data contained within each force-volume dataset. These data were analyzed to ensure normal distribution, indicating uniform contact area between the drug probe and the smooth substrate surfaces. Arithmetic mean and standard deviation were measured to produce CAB plots for the interactions of the different batches of FP with both lactose monohydrate and SX.

### Preparation of Powder Formulations

Binary powder blends (4 g) were manufactured using lactose monohydrate and 1.0% *w*/*w* FP (day 0, LH, HH, or HT). A pre-weighed amount of lactose monohydrate (3.96 g) was initially passed through an 850-μm aperture sieve to break any large agglomerates which may have formed during storage. A quarter of the mass of the lactose monohydrate required was transferred to a stainless steel cylindrical vessel with an internal diameter of 100 mm and a height of 150 mm, and all the FP (40 mg) were sandwiched with another quarter of the sieved lactose monohydrate. This was mixed in a T2F Turbula® mixer (Wily A Bachofen AG, Basel, Switzerland) for 10 min at 46 rpm. The remaining half of the lactose monohydrate was then added and mixed for a further 45 min at 46 rpm. Upon blending, formulations were passed through a 250-μm sieve and stored at 20±2°C and 44% RH for at least 48 h before the content uniformity of the blends was assayed. Tertiary powder blends containing FP (1.0% *w*/*w*), SX (0.2% *w*/*w* SX base), and lactose monohydrate were similarly prepared by sandwiching 40 mg of FP and 8 mg of SX between one half of the lactose monohydrate then mixed for 10 min at 46 rpm and then the remaining one half of the lactose added and mixed for a further 45 min at 46 rpm.

Following content uniformity testing, 25±1 mg of the formulated blend was loaded into size 3 hydroxypropylmethyl cellulose (HPMC, Shionogi Qualicaps, Madrid, Spain) capsules. The targeted dose of the binary formulations was 250 μg of FP per 25-mg fill weight. For the tertiary formulations, the targeted dose of FP and SX were 250 μg and 50 μg, respectively, per 25-mg fill weight. The filled capsules were stored at 20±2°C and 44% RH for 24 h prior to *in vitro* testing to ensure dissipation of any electrostatic charges that may have been introduced during processing.

### HPLC Analysis of Fluticasone Propionate and Salmeterol Xinafoate

The drug content was quantified using HPLC. For the determination of drug content in FP binary formulations, the HPLC method consisted of a pump coupled to an autosampler and multiwavelength UV detector (Agilent 1200, Wokingham, UK) with a wavelength set at 235 nm. The pump flow rate was set to 1.5 mL/min through a Hypersil ODS-$C_{18}$ column (Fisher Scientific, Loughborough, UK, column length of 250 mm, internal diameter of 4.6 mm, and particle size of the packing material of 5 μm), which was placed in a column oven (Agilent, Wokingham, UK) set to 40°C. The injection volume was 20 μL. The mobile phase consisted of methanol, acetonitrile, and water (45:35:20% *v*/*v*). The elution time for the FP peak using this method was 3.4 min.

For the drug content determination of FP and SX in combination formulations, the HPLC method used a flow rate of 1.0 mL/min through a Hypersil BDS-$C_{18}$ column (Fisher Scientific, Loughborough, UK, column length of 250 mm, internal diameter of 4.0 mm, and particle size of the packing material of 5 μm) placed in a column oven at 40°C, with an injection volume of 20 μL. The mobile phase consisted of 75:25% *v*/*v* methanol/0.6% *w*/*v* aqueous ammonium acetate. The UV detection wavelength was set to 228 nm and the elution times for xinafoic acid, salmeterol base, and fluticasone propionate was 2.28, 4.43, and 5.43 min, respectively.

For both methods, a linear regression analysis was used for the assessment of the HPLC calibration. Quantification

was carried out by an external standard method, and linearity was verified ($R^2 \geq 0.998$) for all compounds between 0.05 and 50 μg/mL.

### Content Uniformity

Ten random samples of 25±1 mg, from different areas of the powder bed, were weighed and dissolved in 50 mL of mobile phase. The amount of drug in each sample was obtained from HPLC assay and the content uniformity was expressed as a relative standard deviation (%RSD).

### *In Vitro* Aerosolization Analysis

*In vitro* testing was performed using a Next Generation Impactor (NGI, Copley Scientific, Nottingham, UK) with a pre-separator, which was connected to two vacuum pumps (Copley Scientific, Nottingham, UK) to create critical (sonic) flow. The pre-separator contained 15 mL of mobile phase. The NGI cups were coated with 1% *v/v* silicone oil in hexane to eliminate any particle bounce. For each experiment, two capsules of the same blend were discharged into the NGI at 55 L/min for 4.4 s, equivalent to a total volume of 4 L. Prior to each test, the flow rate was verified using a digital flow meter (DFM 2000, Copley Scientific, Nottingham, UK). The amount of API deposited on each part of the NGI was determined by HPLC. This protocol was repeated three times for each formulation. The mass median aerodynamic diameter (MMAD), geometric standard deviation (GSD), fine particle dose (FPD), and impactor stage mass (ISM) were determined for each case. In all cascade impactor tests conducted, the mass balance was within ±15% of the total recovered dose.

### Statistical Analysis

Statistical analysis between different populations was carried out using one-way analysis of variance. Comparison of the mean values was performed by Tukey's multiple comparison. All statistical analyses were performed using GraphPad Prism software (GraphPad Software Inc, California, USA). Error bars in graphical representations of data show ±standard deviation (SD) in all cases.

## RESULTS AND DISCUSSION

To investigate the effect of controlled environmental lagering on the structural relaxation behavior of micronized FP, a range of physicochemical properties was systematically evaluated under different storage conditions and over predefined time periods. Colloidal probe CAB-SPM was then utilized to provide a more functional measurement of the influence of these physicochemical properties on the surface interfacial interaction of conditioned FP samples with FP, SX, and lactose monohydrate substrate surfaces. These data were further compared to the *in vitro* performance of binary and tertiary DPI formulations containing the micronized (used as received) and lagered FP samples.

### Physicochemical Characterization

Representative XRPD profiles of the day 0, LH90, HH90, and HT FP samples are shown in Fig. 1 (other time point traces are not shown). The presence of distinct peaks in the XRPD profiles between 10° and 40° angle 2θ for all samples suggested that all FP samples were of the same polymorphic form and that conditioning of FP samples under the environments and periods chosen in this study did not alter the crystalline form (1). There was, however, a broad diffuse peak below 10° angle 2θ for both the LH90 and HH90 samples. The origin of this peak was not fully understood but might suggest either incorporation of greater randomness within the crystalline structure or possible changes in preferred orientation of the crystallites upon packing into the instrument caused by extended exposure to low and high relative humidity.

Representative DSC thermographs of the day 0, LH90, HH90, and HT FP samples are shown in Fig. 2. Thermal analysis of all samples (other time point traces not shown) indicated that all materials had an onset of melting at approximately 295°C, which was related to the melting point for form I of FP (14). Again, the DSC data further supported the same polymorphic form of all FP samples.

PSD of day 0 and all lagered FP samples are summarized in Table II. These data showed that while the PSD was relatively insensitive to lagering at HT, lagering of FP under controlled humidity conditions led to some observable changes in the PSD of lagered FP samples. For example, upon exposure to LH, the $d_{50}$ of FP showed an increase at 30 days (2.74 μm), followed by a decrease at 60 days (2.18 μm) and an increase at 90 days (2.68 μm) where the $d_{50}$ remained below the initial value (2.41 μm). A similar qualitative trend was observed for HH samples.

The corresponding surface areas measured by laser diffraction and BET as well as the $R_a$ of the FP samples are tabulated in Table II. The SSA measurements followed, in most cases, a similar qualitative trend to that observed in the particle size and $S_v$ measurements by laser diffraction. For example, upon exposure to 33% RH, there were noticeable increase and subsequent decrease in the SSA at 60 and 90 days, respectively, with respect to SSA at 30 days.

However, an anomalous finding was observed for the HH90 FP sample. Unlike the particle size and $S_v$ data of

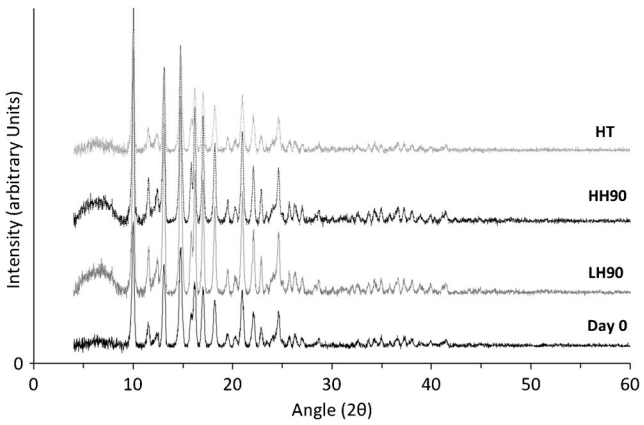


**Fig. 1.** X-ray powder diffraction profiles for the day 0, LH90, HH90, and HT FP samples

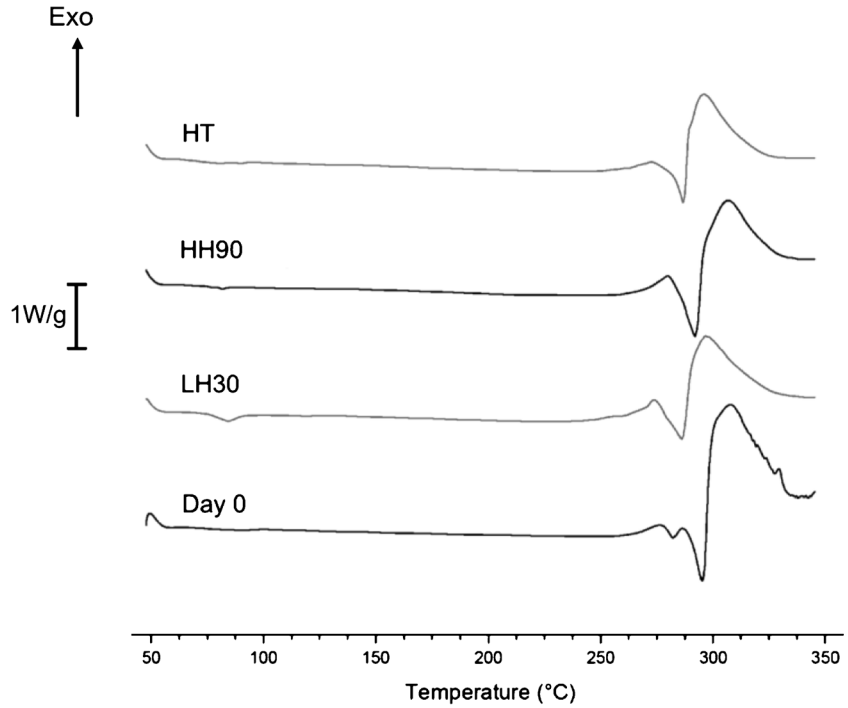


**Fig. 2.** Differential scanning calorimetry (DSC) thermographs for the day 0, LH90, HH90 and HT FP samples

HH30 and HH60, the HH90 FP sample showed a significant decrease in the SSA accompanied by a noticeably smaller value of $R_a$ with respect to all other FP samples. This observation indicated a marked reduction in the surface roughness of the HH90 FP sample. These data suggested that the morphology of the HH90 FP sample differed considerably from the other lagered FP samples.

Representative SEM images of the day 0, HT, LH90, and HH90 FP samples are shown in Fig. 3. With the limited spatial resolution of the SEM, it is difficult to quantitatively discern morphological and surface roughness differences of the day 0 FP sample from the HT and LH90 FP samples. However, it appeared that lagering under high humidity conditions (HH90) created a noticeable change in morphology, resulting in increased surface smoothening (Fig. 3d) consistent with the decrease observed in the SSA and $R_a$ measurements. However, these topographical changes were not apparent for HH30 and HH60 FP samples (data not shown). The surface transformation of the HH90 FP samples suggested that lagering at high humidity (>75% RH) for an extended period of time ($60 < t < 90$ days) may provide the conditions to overcome the activation energy required for the molecular mobility in the disordered regions to undergo surface reconstruction.

## Post-micronization Conditioning Effects on Amorphous Content and Interfacial Forces of FP Samples

The amorphous contents by TAM for the FP samples are summarized in Table II. These data indicated that all lagering conditions led to a lowering in the amorphous content. Lagering under high temperature (*i.e.*, HT FP sample) reduced the amorphous content to below the limit of quantification (LOQ) of the analytical method. Under ambient temperatures, the partial water vapor pressure surrounding the FP powder and the period of exposure also had a direct effect on the amorphous content. Under high humidity conditions, there was a sharp decrease in the amorphous content of the HH30 and HH60 FP samples. In contrast, under low

**Table II.** Physicochemical Measurements of Micronized (Day 0) and Lagered Samples of FP

| FP sample | $d_{10}$ (μm) | $d_{50}$ (μm) | $d_{90}$ (μm) | $S_v$ ($m^2/cm^3$) | SSA ($m^2/g$) | $R_a$ | AC (%) | CAB ratio wrt Lactose | CAB Ratio wrt SX |
|---|---|---|---|---|---|---|---|---|---|
| Day 0 | 1.12±0.01 | 2.41±0.02 | 4.37±0.02 | 2.29 | 7.54±0.27 | 3.30 | 5.05±0.20 | 1.09±0.01 | 2.00±0.03 |
| LH30 | 1.28±0.02 | 2.74±0.01 | 4.99±0.03 | 2.01 | 7.43±0.31 | 3.70 | 4.89±0.18 | 1.04±0.02 | 1.83±0.01 |
| LH60 | 0.96±0.01 | 2.18±0.01 | 4.03±0.01 | 2.55 | 7.98±0.18 | 3.13 | 4.34±0.21 | 0.92±0.01 | 0.80±0.02 |
| LH90 | 1.29±0.01 | 2.68±0.03 | 4.86±0.01 | 2.02 | 7.40±0.22 | 3.66 | 1.12±0.20 | 0.88±0.02 | 0.52±0.02 |
| HH30 | 1.19±0.03 | 2.57±0.01 | 4.72±0.02 | 2.14 | 7.88±0.11 | 3.68 | 2.77±0.18 | 0.76±0.03 | 1.44±0.02 |
| HH60 | 0.99±0.03 | 2.22±0.02 | 4.09±0.02 | 2.49 | 7.49±0.21 | 3.01 | 1.88±0.21 | 0.93±0.02 | 0.85±0.03 |
| HH90 | 1.08±0.01 | 2.33±0.02 | 4.22±0.02 | 2.36 | 4.90±0.17 | 2.07 | 1.29±0.20 | 1.15±0.02 | 0.64±0.01 |
| HT | 1.14±0.02 | 2.40±0.01 | 4.28±0.03 | 2.27 | 7.01±0.33 | 3.08 | <LOQ | 0.74±0.01 | 1.17±0.02 |

*FP* fluticasone propionate, *SSA* specific surface area, *CAB* cohesive-adhesive balance, *SX* salmeterol xinafoate, *LH* low humidity, *HH* high humidity, *HT* high temperature, *AC* amorphous content

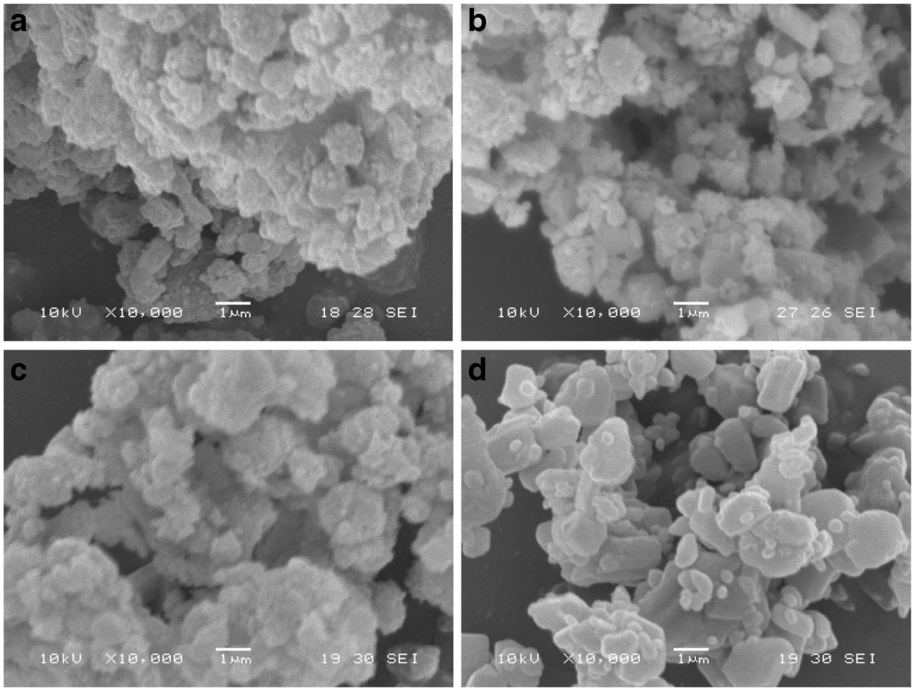


**Fig. 3.** Scanning electron micrographs for the day 0 (**a**), HT (**b**), LH90 (**c**), and HH90 (**d**) FP samples

humidity, there was only a minor decrease in the amorphous content of the LH30 and LH60 FP samples. However, the amorphous contents of the LH90 and HH90 samples were low. Interestingly, while the relaxation pathway of the amorphous disorder was different for FP conditioning under 33% RH and 75% RH, as suggested in the previous physiochemical and SEM data, the amorphous content at 90 days was similar for the both conditions, which was around 1.0%.

### Post-micronization Conditioning Effects on Interfacial Forces

The influence of different lagering conditions on the surface interfacial forces of the micronized and lagered FP samples was investigated by CAB analysis. The individual CAB plots of the FP samples with respect to both lactose monohydrate and SX are provided as supplemental materials (Figs. S1–S3). A summary plot of the CAB values *versus* low and high humidity lagering conditions are plotted in Fig. 4.

The CAB ratios with respect to lactose monohydrate for the low humidity lagering conditions indicated a shift from a slightly cohesive-led interaction (FP-FP, CAB ratio >1.0) for the micronized FP to an adhesive-led system (FP-lactose, CAB ratio <1.0) as shown in Fig. S1, Fig. 4, and Table II. In other words, these data suggested that the adhesion of FP to lactose monohydrate increased upon extended exposure of FP to low humidity conditions. The CAB ratios of the low humidity lagered FP samples with SX (Table II) also indicated that a significant change in the interfacial forces between FP and SX substrates occurred upon lagering. The cohesive nature of the day 0 FP sample, which was twofold greater than its affinity to SX, only slightly decreased for the LH30 sample. However, upon lagering at low humidity for 60 days, the CAB measurements demonstrated a significant ($p<0.02$) shift from a highly cohesive-led system to an adhesive-led (FP-SX>FP-FP) system. This shift to an adhesive (FP-SX)-led system continued for the LH90 FP sample, with the 90-day lagered FP sample shifting the balance of forces to an approximately twofold greater adhesive (FP-SX) interaction than its cohesive (FP-FP) interaction. These data indicated that lagering micronized FP sample for 90 days at 33% RH increased the adhesive interaction to the SX by about fourfold with respect to the as-received micronized FP.

The low sensitivity of the FP-lactose CAB interactions and the highly sensitive nature of the FP-SX CAB to surface chemistry of the secondary processed FP have been observed previously by Kubavat et. al. (1). They also showed that different solvent and anti-solvent conditions during primary crystallization conditions could directly affect the interfacial surface chemistry of the secondary processed FP.

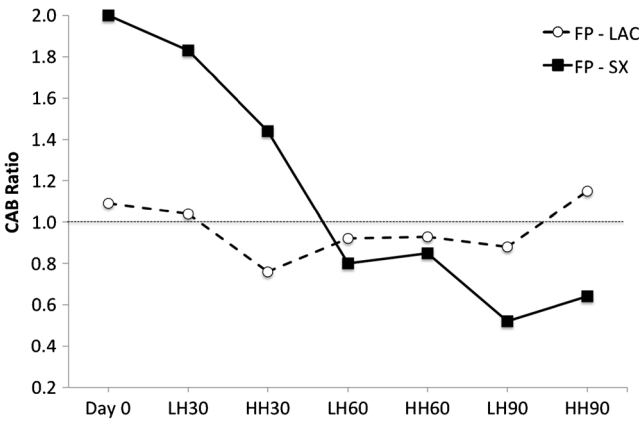


**Fig. 4.** Variations in the CAB ratios with respect to lactose monohydrate and SX of micronized FP particles lagered under low and high relative humidity at 30-, 60-, and 90-day time points

A similar trend in the FP-SX CAB measurements was observed upon lagering under high humidity conditions (Fig. 4, Table II). However, the FP-lactose CAB measurements did not follow a similar trend as the low humidity lagered FP samples. As reflected in the CAB ratios relisted in Table II, initial exposure to elevated humidity increased the adhesive tendency of FP to lactose monohydrate (HH30) to a greater extent than the 90-day exposure at 33% RH (*i.e.*, LH90 FP sample). However, both 60- and 90-day exposures to 75% RH subsequently reduced the adhesive tendency of the lagered FP samples to lactose monohydrate. As a result, the HH90 sample exhibited a greater cohesive tendency than its interaction with lactose monohydrate. Such findings have been previously seen between a partially and fully mechanically relaxed new chemical entity (15). It should also be noted that in Table II, the HH90 FP sample showed both the greatest cohesive tendency with respect to lactose monohydrate and a relatively high adhesive tendency to SX. This unique combination of changes in the interactive force measurements is most likely due to the structural reconstruction of the FP surface as indicated by the marked decrease in SSA and rugosity values of the HH90 FP.

High-temperature conditioning of FP at 60°C led to the greatest increase in the adhesive tendency of the FP to lactose monohydrate, with respect to the cohesive interaction (Table II). However, for the FP-SX CAB measurements, while exhibiting a significant ($p<0.05$) decrease in cohesiveness (Table II, Fig. S3), the HT sample failed to shift the dominant force to an adhesive-led system that was observed with lagered FP samples under high and low humidity conditions.

## Drug Content Uniformity

The relative standard deviation (RSD) measurements of the drug content for binary and tertiary DPI formulations containing micronized and lagered FP are shown in Table III. For all binary DPI formulations, the RSDs were ≤2.5%, indicating homogeneity of the prepared mixtures. In the tertiary DPI formulations, the RSDs for FP were ≤3%, while for SX were ≤5.5%, which suggested a homogeneous distribution of the two active ingredients in the formulated mixtures.

## *In vitro* Aerosolization Performance of Binary DPI Formulations

The *in vitro* APSD characterization of binary DPI formulations containing lactose monohydrate and micronized or lagered FP sample are summarized in Table III. The MMAD and FPM are also plotted as a function of LH and HH lagering conditions in Fig. 5, together with a plot of their respective FP-lactose CAB values. For the HT FP sample, there was a

**Table III.** *In Vitro* Formulation Performance, as Measured by the Mass Balance (MB), Impactor Stage Mass (ISM), Mass Median Aerodynamic Diameter (MMAD), Geometric Standard Deviation (GSD) and Fine Particle Mass ($FPM_{<5\mu m}$), from the Aerosolization of Binary and Tertiary DPI Formulations of Freshly Micronized and Lagered FP Samples ($n=3$). Note that the large SDs in some APSD Data Below Were Related to Variations in Device Losses Between the Repeated Runs

| Sample | %RSD | >MB (%) | ISM (μg±SD) | MMAD (μm±SD) | GSD (μm±SD) | FPM (μg±SD) |
|---|---|---|---|---|---|---|
| Binary wrt FP | | | | | | |
| Day 0 | 1.3 | 92.6 | 32.07±0.90 | 3.80±0.03 | 2.01±0.00 | 29.02±0.80 |
| LH30 | 0.9 | 103.8 | 35.39±8.14 | 3.65±0.04 | 2.04±0.02 | 31.60±7.57 |
| LH60 | 1.0 | 91.1 | 48.58±0.73 | 4.22±0.01 | 2.03±0.00 | 46.74±0.40 |
| LH90 | 1.8 | 105.4 | 57.68±0.50 | 4.24±0.01 | 2.05±0.01 | 55.67±0.37 |
| HH30 | 1.0 | 97.0 | 29.01±0.39 | 4.28±0.01 | 2.15±0.02 | 28.82±0.34 |
| HH60 | 1.6 | 92.4 | 36.50±1.38 | 4.08±0.13 | 2.00±0.02 | 34.06±0.58 |
| HH90 | 2.2 | 98.8 | 47.16±0.67 | 3.92±0.01 | 2.01±0.00 | 43.27±0.57 |
| HT | 1.4 | 93.4 | 37.26±1.06 | 4.06±0.05 | 1.99±0.02 | 34.88±1.11 |
| Tertiary wrt FP | | | | | | |
| Day 0 | 3.0 | 90.6 | 36.18±3.77 | 4.76±0.26 | 2.04±0.01 | 37.19±2.57 |
| LH30 | 1.6 | 98.4 | 46.03±8.13 | 4.37±0.32 | 2.01±0.07 | 43.89±9.86 |
| LH60 | 1.4 | 92.0 | 40.61±2.17 | 4.54±0.09 | 1.93±0.04 | 39.59±1.02 |
| LH90 | 2.2 | 93.2 | 60.48±0.30 | 3.90±0.02 | 2.01±0.02 | 55.50±0.04 |
| HH30 | 1.0 | 99.1 | 32.75±0.36 | 4.28±0.02 | 1.91±0.02 | 30.84±0.16 |
| HH60 | 1.3 | 90.6 | 43.70±6.20 | 3.62±0.03 | 1.91±0.02 | 37.70±5.29 |
| HH90 | 1.9 | 97.0 | 52.79±0.65 | 3.53±0.01 | 1.94±0.00 | 45.44±0.57 |
| HT | 2.1 | 91.5 | 29.78±1.71 | 4.08±0.26 | 1.87±0.12 | 27.14±3.42 |
| Tertiary wrt SX | | | | | | |
| Day 0 | 5.5 | 91.3 | 8.09±0.57 | 3.77±0.05 | 2.18±0.06 | 7.60±0.38 |
| LH30 | 2.8 | 97.1 | 11.02±1.66 | 3.24±0.17 | 2.15±0.01 | 9.64±1.60 |
| LH60 | 1.9 | 95.2 | 11.43±0.11 | 3.00±0.12 | 2.75±0.33 | 10.56±0.46 |
| LH90 | 2.1 | 97.4 | 11.87±0.19 | 3.02±0.07 | 2.47±0.04 | 10.72±0.12 |
| HH30 | 2.7 | 91.7 | 10.07±1.36 | 2.97±0.05 | 2.06±0.01 | 8.32±0.38 |
| HH60 | 2.5 | 96.5 | 10.71±0.19 | 2.71±0.19 | 2.48±0.05 | 9.07±0.42 |
| HH90 | 2.6 | 97.4 | 14.57±0.63 | 2.29±0.10 | 2.80±0.06 | 12.32±0.40 |
| HT | 1.6 | 96.8 | 8.53±0.57 | 2.80±0.06 | 2.57±0.14 | 6.63±0.37 |

*FP* fluticasone propionate, *RSD* relative standard deviation, *LH* low humidity, *HH* high humidity, *HT* high temperature, *SX* salmeterol xinafoate, *SD* standard deviation

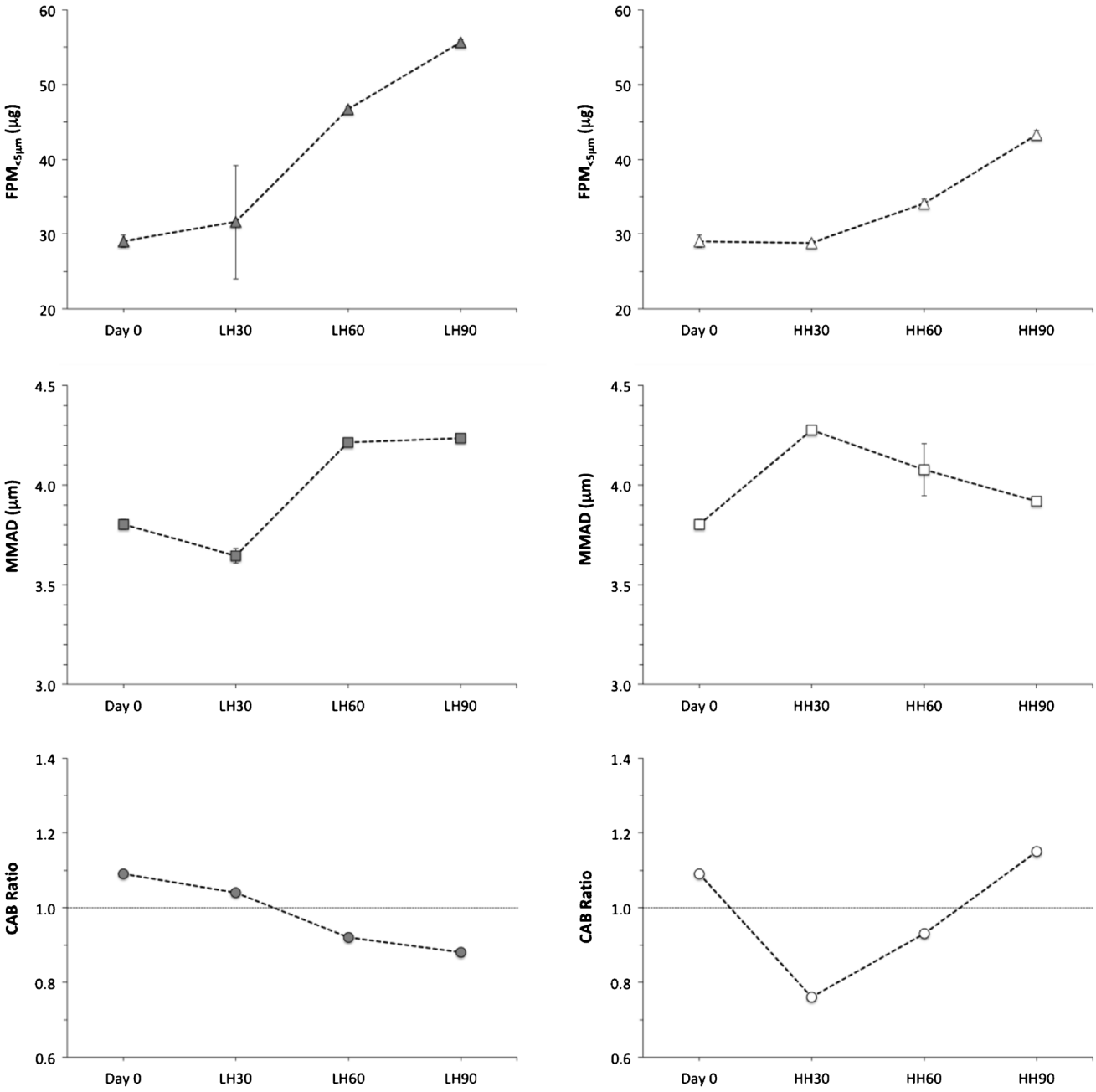


**Fig. 5.** *In vitro* aerosolization performance of FP in binary DPI formulations upon lagering a batch of micronized FP under low and high relative humidity for 30, 60, and 90 days. The corresponding CAB ratios with respect to lactose monohydrate under such conditions are also plotted

significant ($p<0.05$) increase in the FPM and MMAD with respect to the day 0 FP sample. Similarly, there was also a significant ($p<0.05$) increase in MMAD and FPM of the LH FP samples over 60 and 90 days, with respect to the day 0 and LH30 samples.

These differences in APSD of the HT and LH FP samples did not appear to be directly related to changes in the material physical properties (*e.g.*, particle size and surface area). The CAB measurements, however, suggested that the balance of forces for the LH FP samples shifted from being cohesive at day 0 and 30-day exposure to being adhesive following lagering for 60 and 90 days. This was also observed from the day 0 to HT FP sample. Such a shift in the nature of interaction force corresponds with an increase in MMAD of the formulations, which might be related to the formation of API/fines agglomerates owing to the higher adhesive affinity of LH60 and LH90 FP samples to lactose monohydrate fines. It should be noted that with the high levels of intrinsic lactose monohydrate fines (<4.5 μm) present in the ML001 grade of lactose (ca. 10–15% *w/w*), a shift in the balance of forces between FP and lactose monohydrate has been previously shown to lead to a greater elutriation and deaggregation efficiency of FP from the coarse carrier surfaces due to stable agglomerate formation with lactose monohydrate fines (16) (17). This mechanism of agglomerate formation, suggested by Jones et al. indicated that a greater adhesive affinity between API and lactose monohydrate led to a significant increase in MMAD and fine particle mass deposited (16).

Lagering FP samples under high humidity conditions for 30, 60, and 90 days also had a significant effect on APSD of the carrier-based DPI formulations (Fig. 5, Table II). Lagering for 30 days under high humidity conditions led to an increase in the MMAD but no significant change in FPM. The increase in MMAD is in agreement with the slight changes in PSD and SSA measurements, and the relative increase in adhesion to the lactose monohydrate, as measured by CAB, which may aid the formation of API/lactose monohydrate fines agglomerates (18) (16). Increasing the period of lagering at the high humidity condition led to an increase in FPM accompanied by a decrease in MMAD (close to but slightly higher than that of the day 0 FP sample) over 90 days. It was not evident that a single parameter was responsible for or could be used to explain this unique change in formulation performance. Nevertheless, the trends observed here might be related to the combined effect of changes in the physical shape, morphology, and interfacial properties of the HH FP particles that may affect the formulation microstructure during processing and formulation performance. Further research is warranted to better understand the fundamental factors and possibly their interactions that influence the performance of binary DPI formulation containing HH30 and HH90 FP samples.

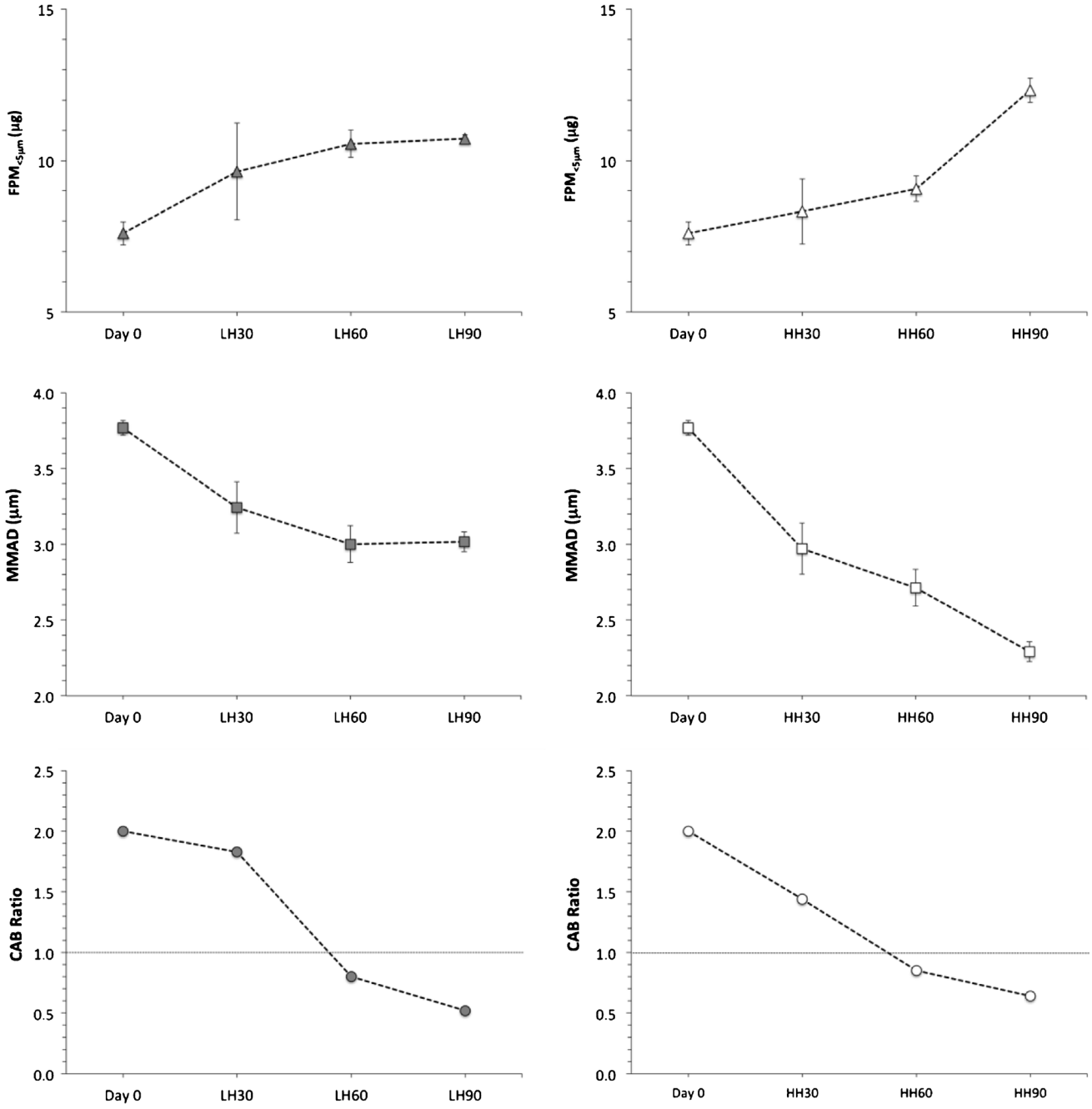


**Fig. 6.** *In vitro* aerosolization performance of SX in combination with FP in tertiary formulations upon lagering a batch of micronized FP under low and high relative humidity for 30, 60, and 90 days. The corresponding CAB ratios with respect to SX under such conditions are also plotted

### *In vitro* Aerosolization Performance of Tertiary DPI Formulations

The *in vitro* APSD characterization of tertiary DPI formulations containing lactose monohydrate, SX, and micronized or lagered FP samples are summarized in Table III. The MMAD and FPM of SX are plotted together with the FP-SX CAB values in Fig. 6. As mentioned above, an aged batch of micronized SX (>12 months) was used. Cohesive-adhesive balance (CAB) measurements indicated that there was no noticeable difference in the interfacial properties of the SX during the duration of the study (the average CAB ratio of SX with respect to lactose monohydrate over the different time points was $1.85 \pm 0.13$).

The aerosolization performance of FP was not significantly ($p > 0.05$) affected by lagering at low humidity over 60 days. However, extended lagering ($60 < t < 90$ days) led to a significant ($p < 0.05$) increase in FPM and a smaller MMAD. Lagering under high humidity, similar to the binary DPI formulations, extended lagering appeared to progressively affect the aerosolization performance of the FP component in the tertiary formulations. However, increasing lagering increased the FPM but decreased the MMAD of the FP component in the presence of SX, whereas for the binary formulation, extended lagering showed an initial marked increase followed by a gradual decrease in FP MMAD and a consistent increase in FP FPM. For the SX component, increasing the period of lagering led to an increase in FPM recovery of SX and a decrease in MMAD of the SX component for LH and HH FP samples.

The aerosolization performance of the tertiary DPI formulations (particularly with respect to the SX component in Fig. 6) appeared to be sensitive to shift in the balance of forces between FP and SX upon FP lagering. As has been indicated in a number of studies, the greater the adhesive tendency between FP and SX, the more significant is the improvement in aerosolization performance of SX (1,16,19). These studies proposed that higher deaggregation efficiency of the SX occurred as a result of the greater propensity of FP and SX to form fine particle agglomerates during blending. Similar observations have also been reported for suspension MDI formulations comprising of FP and SX (20). However, additional studies will be needed to fully understand the complex relationships between the interfacial properties and aerosolization performance for such tertiary systems.

## CONCLUSIONS

The ability to understand and predict interparticulate forces of secondary processing of APIs in DPI systems is critical in our ability to predict and optimize DPI product performance. The relative magnitudes of the cohesive (drug-drug) and adhesive (drug-excipient, drug 1-drug 2 such as FP-SX) forces and how primary and secondary processing of drug materials may directly impact these interparticulate forces is a major research objective. In this study, we have shown that the relative magnitudes of cohesive-to-adhesive forces of secondary processed FP are a direct function of the conditioning environment and duration. While the time to re-equilibrate the FP particles from their unstable amorphous state to the thermodynamically stable crystalline state can be expedited, lagering is an essential parameter requiring controlled conditions of temperature and relative humidity. Unlike high temperature, humidity based conditioning failed to completely eliminate amorphous-related disorders and significantly affected the relative balance of the adhesive and cohesive forces during storage. A significant morphological and topographical change was seen following the conditioning of FP under high humidity for 90 days, suggesting a surface reconstruction event. This study clearly shows that the different post-micronization lagering conditions translated into different interfacial behavior, accompanied by significant changes in product performance characterized by APSD measurements by cascade impaction. However, the fundamental factor(s) and mechanism(s) responsible for the observed differences in product performance are not fully understood for the complex formulations in DPIs investigated here. Therefore, the present study clearly indicates the critical importance and need for more research in understanding the physical, chemical, and interfacial properties of secondary processed materials and their subsequent effect on the product performance.

## REFERENCES


1. Kubavat HA, Shur J, Ruecroft G, Hipkiss D, Price R. Investigation into the influence of primary crystallization conditions on the mechanical properties and secondary processing behaviour of fluticasone propionate for carrier based dry powder inhaler formulations. Pharm Res. 2012;29:994–1006.
2. Ward GH, Schultz RK. Process-induced crystallinity changes in albuterol sulfate and its effect on powder physical stability. Pharm Res. 1995;12:773–9.
3. Joshi V, Dwivedi S, Ward GH. Increase in the specific surface area of budesonide during storage postmicronization. Pharm Res. 2002;19:7–12.
4. Huttenrauch R, Fricke S, Zielke P. Mechanical activation of pharmaceutical systems. Pharm Res. 1985;2:302–6.
5. Brodka-Pfeiffer K, Langguth P, Grass P, Häusler H. Influence of mechanical activation on the physical stability of salbutamol sulphate. Eur J Pharm Biopharm. 2003;56:393–400.
6. Shur J, Pitchayajittipong C, Rogueda P, Price R. Effect of processing history on the surface interfacial properties of budesonide in carrier-based dry-powder inhalers. Ther Deliv. 2013;4:925–37.
7. Wildfong PLD, Hancock BC, Moore MD, Morri KR. Towards an understanding of the structurally based potential for mechanically activated disordering of small molecule organic crystals. J Pharm Sci. 2006;95:2645–56.
8. Colombo I, Grassi G, Grassi M. Drug mechanochemical activation. J Pharm Sci. 2009;98:3961–86.
9. Brodka-Pfeiffer K, Häusler H, Grass P, Langguth P. Conditioning following powder micronization: influence on particle growth of salbutamol sulfate. Drug Dev Ind Pharm. 2003;29:1077–84.
10. Bender H, Graebner H, Schindler K, Trunk M, Watz M.; Boehringer Ingelheim Pharma Gmbh & Co. Kg. Crystalline micronisate, process for the manufacture thereof and use thereof for the preparation of a medicament. US 20040002510 A1. 2004 Jan 1.
11. Riebe MT, Dwivedi SK, Li-Bovet L.; Smithkline Beecham Corporation. Aerosols containing annealed particulate salbutamol and tetrafluoroethane. US6558651 B1. 2003 May 6.
12. Muhrer G, Rasenack N.; Novartis AG. Process for reducing the tendency of a glycopyyronium salt to aggregate during storage. EP2234595 B1. 2012 Nov 28.
13. Begat P, Morton DAV, Staniforth JN, Price R. The cohesive-adhesive balances in dry powder inhaler formulations I: direct quantification by atomic force microscopy. Pharm Res. 2004;21:1591–7.
14. Pitchayajittipong C, Shur J, Price R. Engineering of crystalline combination inhalation particles of a long-acting beta2-agonist and a corticosteroid. Pharm Res. 2009;26:2657–66.
15. Shur J, Kaerger JS, Price R. Effect of surface amorphous content of active pharmaceutical ingredients on the performance of dry

powder inhaler formulations. RDD Europe 2007; Dalby RN, Byron PR, Peart J, Suman J, editors, Davis Healthcare, Rover Grove, Illinois, Vol 1, pp. 341–4.
16. Jones MD, Harris H, Hooton JC, Shur J, King GS, Mathoulin CA, *et al*. An investigation into the relationship between carrier-based dry powder inhalation performance and formulation cohesive-adhesive force balances. Eur J Pharm Biopharm. 2008;69:496–507.
17. Shur J, Harris H, Jones MD, Kaerger JS, Price R. The role of fines in the modification of the fluidization and dispersion mechanism within dry powder inhaler formulations. Pharm Res. 2008;25:1631–40.
18. Begat P, Morton DAV, Staniforth JN, Price R. The cohesive-adhesive balances in dry powder inhaler formulations II: influence on fine particle delivery characteristics. Pharm Res. 2004;21:1826–33.
19. Jones MD, Hooton JC, Dawson ML, Ferrie AR, Price R. An investigation into the dispersion mechanisms of ternary dry powder inhaler formulations by the quantification of interparticulate forces. Pharm Res. 2008;25:337–48.
20. Rogueda PGA, Price R, Smith T, Young PM, Traini D. Particle synergy and aerosol performance in non-aqueous liquid of two combinations metered dose inhalation formulations: an AFM and Raman investigation. J Colloid Interface Sci. 2011;361:649–55.